Disposition of Benzyl Alcohol after Topical Application to Human Skin *In Vitro*

PENPAN SAIYASOMBATI, GERALD B. KASTING

College of Pharmacy, The University of Cincinnati Medical Center, P.O. Box 670004, Cincinnati, Ohio 45267-0004

Received 15 January 2003; revised 20 March 2003; accepted 21 March 2003

ABSTRACT: Dissipation of a volatile compound or mixture from the skin surface after topical application involves both diffusion and evaporation. This report presents a detailed test of a previously described first-order kinetic approach to modeling this problem. Modified Franz diffusion cells fitted with a vapor trap were used to obtain absorption and evaporation data for benzyl alcohol (1% solution in ethanol) after application to human skin *in vitro*. Airflow over the skin surface (v) was controlled in the experiment and accounted for in the model by allowing the evaporation rate constant(s) to vary as a function of v. A linear dependence was found over the working range of the system, 10–100 mL/min. Three kinetic models were developed, all of which satisfactorily correlated cumulative absorption and evaporation results over the full range of v ($n = 120$, $s = 4–5\%$, $r^2 = 0.98–0.99$). One of these was the model presented previously, in which all dissipation occurs from a single skin compartment. However, more details of the evaporation and absorption profiles could be accounted for by means of two-compartment models that explicitly consider the surface film present in the early stages post-application. The latter models seem to be better candidates for describing the time evolution of the volatile mixture evolving from the skin surface after topical application of, e.g., a complex fragrance or perfume. J Pharm Sci 92:2128–2139, 2003

Keywords: absorption; benzyl alcohol; evaporation; fragrance; mathematical model; skin

INTRODUCTION

Fragrances are extensively used in cosmetics and personal care products for either odor masking or aesthetic purposes. These products are intended for daily contact with the skin. Allergic reactions to fragrance ingredients have become of increasing concern to both dermatologists and the cosmetic and toiletries industry. The penetration of an allergen into the skin is required for both induction and elicitation of skin sensitization.[1] Therefore, it is not surprising that the potential of a chemical to act as a contact allergen is related to its ability to penetrate the skin. One of the critical components in skin sensitization risk assessment is the determination of percutaneous absorption of those chemicals identified as potential allergens. Currently, 100% of the topically applied dose from the leave-on products is often assumed for final exposure in assessing skin sensitization risk.[2] This is obviously an overestimate for volatile chemicals.

Computational models for dermal absorption are increasingly used in lieu of animal experiments to estimate absorption of new ingredients. However, the predictive models presently available for this purpose are either steady-state

Correspondence to: Gerald B. Kasting (Telephone: 513-558-1817; Fax: 513-558-0978; E-mail: gerald.kasting@uc.edu)

Journal of Pharmaceutical Sciences, Vol. 92, 2128–2139 (2003)

models[3,4] or are transient absorption models based on steady-state data.[5] Neither accurately represents the exposure conditions common to cosmetic and personal care products. The absorption rate of an ingredient from a small dose applied to skin differs significantly from absorption of a large dose.[6] For volatile materials the situation is even more complex, because a substantial portion of the dose may evaporate rather than absorb into the skin. A reliable computational model for predicting absorption and skin concentrations under these conditions would have great value in the area of dermatological and personal care product development, dermal risk assessment, and the mechanistic understanding of contact allergy.

The investigators have previously proposed a simple, first-order kinetic model for the absorption and evaporation of small amounts of volatile compounds applied to skin.[7] The model was used to interpret evaporation data obtained after application of fragrance mixtures applied to human volar forearm *in vivo*.[8] This report presents a detailed test of an extended first-order kinetic approach using combined absorption and evaporation data obtained after application of a single fragrance ingredient, benzyl alcohol, to human skin *in vitro*. Benzyl alcohol penetrates skin to a significant extent[9–13] and is one of the more frequently reported contact allergens,[14] possibly because of its widespread use in both fragrance and preservative systems for cosmetic products. However, it is not considered a high-risk ingredient.

We show below that the previous one-compartment kinetic model[7] satisfactorily correlates the absorbed and evaporated fractions of benzyl alcohol from human skin *in vitro* with surface airflow over a wide range of airflow conditions. However, the detailed kinetics of these processes are missed by this approach. Two different two-compartment models are presented that provide significant improvements in this area by explicitly considering the surface film present in the early stages of evaporation. Thus, they represent an important step in the understanding and eventual prediction of skin absorption/evaporation phenomena.

Theory

The absorption of a volatile compound or mixture from the skin surface is a combined diffusion/evaporation process. Immediately after application, transport presumably occurs from a surface film, the components of which evaporate and absorb into the stratum corneum at different rates depending on their physicochemical properties. Highly volatile and skin permeable components such as ethanol dissipate rapidly, whereas less volatile, higher molecular weight compounds may reside on the skin surface for a substantial period of time. For mixtures, rapid evaporation of the more volatile compounds may lead to significant surface cooling, delaying the evaporation of other components by depressing their vapor pressure. Ingredients in solution may interact with one another, thereby altering activity coefficients. Hence, a complete description of the evaporation process involves the solution of a combined heat and mass-transport problem involving concentrated solutions with multiple ingredient interactions. Skin absorption makes the problem even more complex, because skin is a heterogeneous membrane composed of multiple layers of substantial complexity.[4]

In this report, as in the previous one,[7] we have adopted the philosophy of offering the simplest solution to the problem that provides insight into the operative physical processes and has the potential to make useful predictions. We begin by briefly reviewing the one-compartment kinetic model, Model 1.[7] A schematic diagram is shown in Figure 1a. The skin is assumed to be a single, well-stirred compartment that rapidly incorporates a topically applied ingredient. The amount of the ingredient remaining in the skin at time t after application of amount A_0 at time zero is

$$A(t) = A_0 e^{-(k_1+k_2)t} \tag{1}$$

where k_1 is the evaporation rate constant and k_2 is the absorption rate constant. The rate constants for each compound are functions of temperature (T), surface airflow (v), and three physico-chemical properties: vapor pressure (P_{vp}), molecular weight (MW), and lipid solubility (S_{lip}). The latter is taken to be solubility in n-octanol, expressed as the product of water solubility (S_w) and octanol-water partition-coefficient (K_{oct}). Each property is expressed in dimensionless, or "reduced," form by dividing by a characteristic value; thus,

$$k_1 = k_1^v \cdot P_{vpr}/(K_{oct} \cdot S_w)_r \tag{2}$$

$$k_2 = k_2^T \cdot MW_r^{-27} \tag{3}$$

In eqs. (2) and (3), $P_{vpr} = P_{vp}/1$ torr, $(K_{oct} \cdot S_w)_r = (K_{oct} \cdot S_w)/1000$ g cm^{-3}, $MW_r = MW/100$ Da, and k_1^v and k_2^T are proportionality constants dependent on surface airflow and temperature,

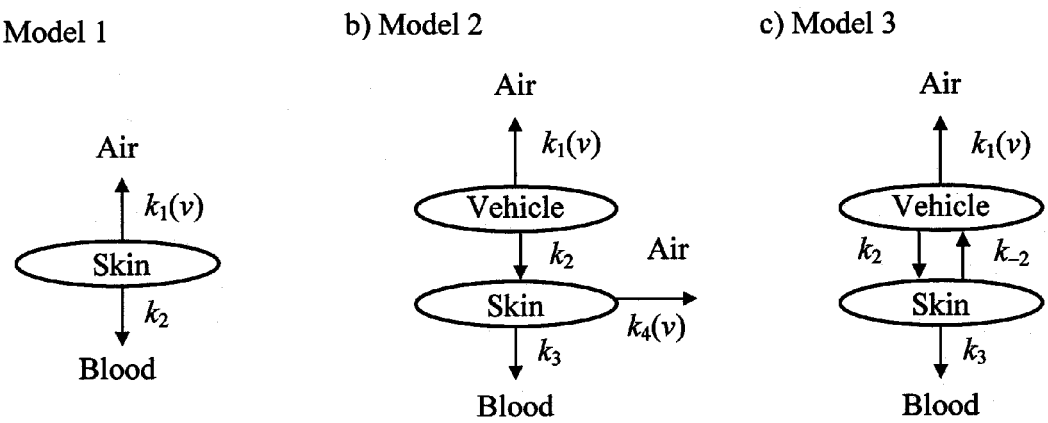

Figure 1. Schematic diagrams for compartmental models of skin disposition. (a) One compartment (Model 1), (b) two compartments with evaporation from vehicle and skin (Model 2), and (c) two compartments with evaporation from vehicle only (Model 3).

respectively. The fractions evaporated and absorbed after a long time are

$$f_{\text{evap}} = \frac{k_1}{k_1 + k_2} = \frac{x_r}{k + x_r} \tag{4}$$

$$f_{\text{abs}} = \frac{k_2}{k_1 + k_2} = \frac{k}{k + x_r} \tag{5}$$

where $k = k_2^T/k_1^v$ and $x_r = P_{\text{vpr}}\text{MW}_r^b/(K_{\text{oct}} \cdot S_w)_r$.

Equation 4 was used to correlate the evaporation of 10–11 perfume ingredients applied as two different mixtures to human skin *in vivo*.[8] Squared correlation coefficients, r^2, of 0.74 and 0.52 for fits of eq. (4) to the evaporated fractions were obtained, with standard deviations of 12 and 14%, respectively. Significant correlations of physical properties to the rate constants k_1 and k_2 were obtained according to eqs. (2) and (3). However, curvature of the semi-logarithmic plots of evaporation rate versus time indicated that the evaporation rates of some ingredients could not be described by the single exponential decay constant, $k_1 + k_2$, given in eq. (1). The curvature was suggestive of higher initial evaporation rates, as might be obtained from a surface film.

The previous analysis and the experimental results presented below suggest that an improved absorption/evaporation model might be obtained by including a surface film. Two ways of doing this are shown in Figure 1b and c. Both of these diagrams depict two well-stirred compartments—one representing the surface film (or vehicle), the other representing the skin. If the analysis is restricted to compounds of moderate lipophilicity such as ethanol, benzyl alcohol, or most fragrance ingredients, the skin compartment may be considered to be the stratum corneum lipids, which form the primary barrier to penetration of such materials.[4,5] In Model 2 (Fig. 1b), evaporation is assumed to occur first from the vehicle, which is rapidly depleted by the combination of this process with partitioning into the skin. During the depletion process, the volume of the vehicle layer continuously decreases until the layer finally disappears. Subsequent evaporation and absorption occur from the skin (or stratum corneum) compartment. The characterization of evaporation as two distinct processes makes sense only if the time constant for dissipation of the surface film, $1/(k_1 + k_2)$, is much less than that for the skin compartment, $1/(k_3 + k_4)$. If this is not the case, then Model 3 (Fig. 1c) should be considered. In Model 3, the vehicle layer remains as a discrete film until the last of the components has completely dissipated. Either of these scenarios might occur in practice, with more volatile and/or skin permeable films dissipating according to Model 2 and less volatile/permeable films dissipating according to Model 3. We show below that Models 2 and 3 provide comparable descriptions of the dissipation of benzyl alcohol applied to skin in ethanol, and that these descriptions are more accurate at early times than that provided by Model 1.

It is possible to construct two-compartment models having additional rate constants involving reverse transfer from the blood or skin, or to add an additional compartment representing the viable skin layers.[15] Such additions would almost certainly improve the ability of the models to correlate data. However, unless the parameters associated with the additional features can be independently determined, the predictive power is likely to decrease. In the present analysis, we have forgone

these elaborations and focused on the extent to which a four-parameter absorption/evaporation model (Model 2 or 3) can improve upon the description offered by a two-parameter model (Model 1). Of particular interest is the form of the surface airflow dependence for the evaporation rate coefficient k_1^v (eq. 2) and its analogs in the two-compartment models.

The rate equations for Models 2 and 3 are readily solved using standard methods for linear pharmacokinetic models.[16] The solutions are given in the Appendix. The integrated equations representing the amount of compound in air [the evaporated amount, eqs. (A.3) and (A.11)] and in blood [the absorbed amount, eqs. (A.6) and (A.14)] will be used to model the data from the *in vitro* evaporation/penetration studies. The physical properties dependencies of the rate constants [see eqs. (2) and (3)] will not be considered in this report, because only one compound was studied. Additional analyses of these factors have been conducted[17] and will be reported separately. However, the airflow dependence of the parameters $k_1(v)$ and $k_4(v)$ in the *in vitro* diffusion/evaporation cells will be examined. Two simple functional forms are proposed (k_1 and k_4 are treated identically):

$$k_1(v) = k_1' \cdot v \tag{6}$$

and

$$k_1(v) = k_1'' \cdot \frac{v}{v+b} \tag{7}$$

Equation (6) corresponds to a laminar flow model in which the thickness of the unstirred air layer limiting diffusion from the film is inversely proportional to the air velocity v. Equation 7 is an extension of the laminar flow model that allows for a component of the evaporative mass transfer resistance, i.e., a surface resistance $R_1 = 1/k_1''$ that is independent of v. At low airflows, eqs. (6) and (7) yield equivalent results, with $k_1' = k_1''/b$.

EXPERIMENTAL

Chemicals

7-^{14}C-Benzyl alcohol (55 mCi/mmol; 0.1 mCi/mL in ethanol) and unlabeled benzyl alcohol (CAS no. 100-51-6), 99% (GC assay) were purchased from Moravek Biochemicals (Brea, CA) and Sigma-Aldrich (St. Louis, MO), respectively. The radiochemical purity of the ^{14}C-benzyl alcohol was stated by the manufacturer to be 98.3%.

The physical properties of benzyl alcohol are as follows: molecular weight (MW) = 108.1 Da, vapor pressure (P_{vp}) at 30°C = 0.0847 mmHg,[18] water solubility (S_w) at 30°C = 44.7 g/L[19] and log octanol-water partition coefficient ($\log K_{oct}$) = 1.1.[20]

Dose Solution

In each experiment, 10 μL of a 1% w/v ^{14}C-benzyl alcohol in ethanol (50 μCi/mL) was applied to each 0.79 cm^2 skin sample, giving an applied benzyl alcohol dose of approximately 127 μg/cm^2. The low surface tension of the ethanolic solution allowed it to spread uniformly on the skin surface before evaporation of the solvent.

Evaporation/Penetration Apparatus

Figure 2 shows the modified Franz diffusion cell used in the evaporation/penetration studies. The cells were custom-made by Dana Enterprises (West Chester, OH). The donor compartment (4 mL) was modified by the addition of a side arm that allowed the passage of air through the cell. The top of the cell was connected to a Tenax TA cartridge (Supelco, St. Louis, MO) via a custom-made glass connector (Dana Enterprises) and an Omnifit® large variable connector for 4–11 mm tubing (Alltech Associates, Inc., Deerfield, IL). A PAS-500 micro air sampling

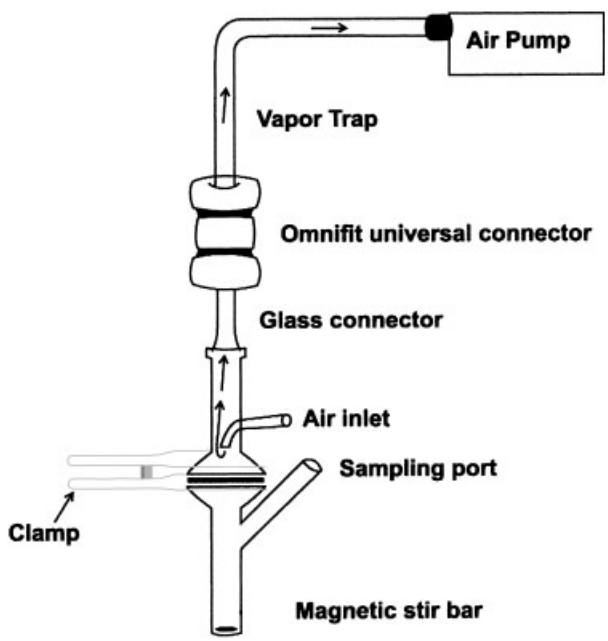

Figure 2. Apparatus for measurement of skin absorption and evaporation *in vitro*.

pump (Spectrex, Redwood City, CA) was connected to the top of the adsorbent tube via silicone tubing (6 mm o.d.) to regulate the airflow through the evaporation cell. Room air was constantly drawn into the inlet of the evaporation cell, over the skin surface, and through the Tenax TA cartridge. The receptor compartment (4.5 mL) was stirred and maintained at 37°C by means of a thermostated heating-stirring module, yielding a skin surface temperature of 30–32°C.[21]

Skin Membrane

Dermatomed human cadaver skin (300 μm) was obtained from the Ohio Valley Tissue and Skin Center (Cincinnati, OH). The frozen skin was cut into small pieces (1.5 × 1.5 cm^2) and thawed in lukewarm, pH 7.4, Dulbecco's phosphate buffered saline (Sigma-Aldrich) containing 0.02% sodium azide before being mounted, epidermal side up, in the evaporation/penetration cell. The receptor compartment was filled with the same buffer solution. The dermal side of the skin was in contact with the receptor solution, and care was taken to ensure that no air bubbles were present.

Skin Permeability Test

Before each study, the integrity of the skin samples was checked using ^3H_2O as described previously.[22] The test involved a 5-min exposure to an excess of ^3H_2O, followed by receptor phase analysis after 1 h. Skin samples used in this study had water permeation values of 0.17–0.57 μg/cm^2. The skin surface was allowed to air dry before application of the ^{14}C-benzyl alcohol solution, as described below.

Evaporation/Penetration Studies

After the receptor solution was replaced twice to remove any residual ^3H_2O, the vapor trap was fitted to the evaporation cell as shown in Figure 2. The system was then connected to the micro air pump to control the flow of air over the skin. After a 1-h equilibration period, the glass connector was removed and the dose solution was applied to the epidermal side of the skin using a 10-μL Hamilton syringe. The system was reconnected immediately after dosing. The exact time of application was noted and designated as time zero for the experiment.

The vapor evaporating from the skin surface was entrained in the air and collected in the Tenax TA cartridge. Vapors were collected continuously. The cartridges were exchanged at 0.08, 0.25, 1.25, 2.25, 4.25, 6.25, and 8 h post-dose. Similarly, the receptor solution was removed and replaced at 0.5, 1, 2, 4, 6, and 8 h post-dose. Radioactivity was quantified by liquid scintillation counting (LSC) using a Beckman LS 6500™ multipurpose scintillation counter (Beckman Coulter, Inc., Fullerton, CA).

After the 8-h samples were collected, the skin was dissolved in 2 mL of Soluene®-350 (Packard BioScience) and analyzed by LSC. The evaporation and penetration cells were separately rinsed with 1 mL of ethanol to remove any residual activity. The rinses were pooled and analyzed by LSC. Studies were conducted at 8 airflow rates ranging from 10 to 100 mL/min. Two trials were conducted at each airflow, with one diffusion cell per trial.

Vapor Collection and Desorption

Tenax TA cartridges collected during the study were desorbed directly into scintillation cocktail using flash heating at 180°C for approximately 10 to 15 min. During the desorption, ultra pure nitrogen gas at 20 mL/min was purged through the cartridges in the direction opposite to that of sample collection. After the desorption, the tubes were reconditioned by passage of 40 mL/min ultra pure nitrogen gas and heating at 10–20°C above the desorption temperature for 20 min.

Data Analysis

The evaporation and absorption rate data were plotted semi-logarithmically versus time. The linear compartmental pharmacokinetic models described earlier (Fig. 1) were fit to the cumulative absorption and evaporation data using nonlinear least squares. Before these fits, the data were normalized by dividing each value by the recovered dose (Table 1, right-hand column), so that the total amount of radioactivity recovered agreed with the model prediction (100%) as $t \rightarrow \infty$. The normalization factor ranged from 90 to 105%. The effect of airflow (v) was accounted for by allowing k_1 and k_4 to vary linearly with v [eq. (6)] or in a saturable manner [eq. (7)]. The parameters in each model were optimized using a computer program of our own design, in the sequence described below. The sum of squared residuals, $SSR = \sum[y_i(obs) - y_i(fit)]^2$, was minimized by means of a parabolic extrapolation

Table 1. Mass Balance for ^{14}C-Benzyl Alcohol Skin Disposition Studies

Airflow Rate (mL/min)	Trial	Dose ($\mu g/cm^2$)	^3H_2O Permeability ($\mu L/cm^2$)	% of Dose				
				Evaporation	Absorption	Skin	Cell Wash	Total Recovery
10	I	138.7	0.51	44.5	48.3	2.9	0.5	96.2
	II		0.44	46.9	55.4	1.9	0.4	104.6
20	I	118.1	0.17	60.6	34.0	1.6	0.2	96.4
	II		0.28	56.2	38.4	1.6	0.2	96.4
30	I	127.1	0.17	75.0	20.5	1.1	0.6	97.2
	II		0.40	70.6	24.8	1.3	0.4	97.1
40	I	129.1	0.26	73.4	15.8	0.7	0.3	90.2
	II		0.38	70.0	25.0	1.4	0.4	96.7
50	I	128.7	0.26	83.2	11.1	0.6	0.4	95.2
	II		0.36	81.0	14.9	0.6	0.6	97.1
65	I	120.8	0.29	69.0	13.5	8.7	0.2	91.4
	II		0.24	81.2	14.2	0.6	0.2	96.1
80	I	139.0	0.24	83.4	10.8	0.6	0.4	95.1
	II		0.57	84.5	16.9	0.7	0.6	102.6
100	I	119.1	0.48	87.2	12.7	0.5	0.1	100.5
	II		0.40	82.3	11.8	0.5	0.2	94.7
							Mean ± SD:	96.7 ± 3.6

algorithm.[23] Reduced chi-square values, $\chi_v^2 = SSR/(n-p)$, where n is the number of observations and p is the number of adjustable parameters, were used to indicate the goodness of fit of the proposed models to experimental data.

Model 1

The optimum values of k_1' [eq. (6)] or k_1'' and b [eq. (7)] were determined by fitting the integrated rate equations to each dataset, then averaging the results. The value of k_2 was then redetermined for each dataset using the optimum value of k_1' (or k_1'' and b). The results for k_2 were then averaged across datasets to give values reported in Table 2. The logic of this procedure is that the evaporation rate constant (k_1) depends only on physicochemical properties of the permeant and the system; hence, it should be less variable than the absorption rate constant (k_2), which depends on skin permeability. By first determining k_1, a better estimate of skin permeability effects on k_2 may be obtained.

Table 2. Regression Parameters for Compartmental Models of Benzyl Alcohol Skin Disposition

Parameters	Units	Model		
		1	2	3
$k_1'(v)$	$h^{-1} \cdot (min/mL)^a$	0.141 ± 0.051	0.194 ± 0.058	0.197 ± 0.057
k_2	h^{-1}	1.6 ± 0.8	3.8 ± 1.5	3.5 ± 1.2
k_{-2}	h^{-1}	—	—	0.6 ± 0.4
k_3	h^{-1}	—	0.9 ± 0.2	0.9 ± 0.3
$k_4'(v)$	$h^{-1} \cdot (min/mL)^a$	—	0.013 ± 0.009	—
n		120	120	120
s	% of dose	4.72	4.66	3.97
r^2		0.9792	0.9807	0.9862
χ_v^2	$(\%\ of\ dose)^2$	22.2	21.6	15.7

[a]Yields h^{-1} when multiplied by v in mL/min [eq. (6)].

Model 2

Parameters were determined sequentially as for Model 1. The order of optimization was k_1', k_2, then (simultaneously) k_3 and k_4'.

Model 3

Parameters were determined sequentially in the order k_1', k_2, then (simultaneously) k_{-2} and k_3.

RESULTS

In vitro skin evaporation and absorption data for ^{14}C-benzyl alcohol at airflows ranging from 10 to 100 mL/min are listed in Tables 3 and 4. The mass balance for these studies is given in Table 1 and the results of the regression analyses for fits of Models 1–3 to the data are shown in Table 2.

The results in Tables 1, 3 and 4 show that evaporation and absorption were strong functions of surface airflow. Higher airflow led to more rapid evaporation and a corresponding increase in cumulative percent evaporated, as would be expected from eqs. (6) or (7). This trend is shown clearly in Figure 3, where cumulative evaporation and absorption over 8 h are plotted versus airflow. Also shown in this plot are the predicted values from Models 1–3, calculated using the regression parameters in Table 2. For these simulations, the linear evaporation rate model, eq. (6), was used to calculate the evaporation rate constants k_1 and k_4. The use of eq. (6) is restricted to interpolation within the range $v = 10–100$ mL/min. Departures from this behavior are expected outside of this range, especially at lower values of v, because a finite evaporation rate is anticipated even in the absence of convective flow ($v = 0$).

Except for the lowest airflow rate, most benzyl alcohol evaporation occurred within 15 min post-dose (Table 3). Absorption was somewhat slower, but most occurred within 2 h (Table 4). By 8 h post-dose, <3% of the applied dose was found in the skin, with one exception (Table 1). The overall recovery of radioactivity in these studies ranged from 90–105% of the applied dose, with a mean value of 97% (Table 1). Thus, the skin disposition of benzyl alcohol was largely complete within 8 h post-dose, and there was little evidence for binding of the compound to the skin.

Representative semi-logarithmic plots of evaporation and absorption rates versus time are shown in Figure 4. Examination of these plots revealed several consistent trends. At low airflow rates (10–30 mL/min), the initial evaporation rate (average rate 0–5 min) was lower than that observed during the next time period, 5–15 min. An example may be seen in Figure 4a. This may be

Table 3. Evaporation of ^{14}C-Benzyl Alcohol from Human Skin In Vitro

Airflow Rate (mL/min)	Trial	Percentage of Dose						
		0.08 h	0.25 h	1.25 h	2.25 h	4.25 h	6.25 h	8 h
10	I	0.95	26.6	15.4	0.86	0.42	0.17	0.09
	II	0.66	18.6	26.0	0.99	0.47	0.15	0.08
20	I	2.5	46.6	9.2	1.1	0.63	0.29	0.23
	II	1.9	35.4	16.5	1.2	0.62	0.34	0.21
30	I	12.6	49.0	11.4	0.97	0.57	0.30	0.18
	II	18.5	43.5	6.6	0.94	0.63	0.29	0.17
40	I	41.4	26.1	4.7	0.59	0.32	0.17	0.10
	II	33.4	29.5	4.4	1.3	0.77	0.28	0.29
50	I	51.0	27.2	3.5	0.58	0.52	0.29	0.14
	II	40.3	34.5	4.7	0.81	0.39	0.15	0.11
65	I	54.7	11.0	2.3	0.43	0.26	0.19	0.11
	II	56.3	20.9	2.8	0.46	0.39	0.22	0.14
80	I	53.2	24.6	4.1	0.86	0.22	0.23	0.10
	II	62.6	18.9	2.1	0.51	0.23	0.12	0.09
100	I	73.0	8.7	4.0	0.70	0.28	0.25	0.17
	II	66.9	11.8	2.3	0.71	0.29	0.20	0.13

Values are expressed as the percentage of the applied dose (Table 1) that evaporated during each time interval.

Table 4. Skin Absorption Data for ^{14}C-Benzyl Alcohol, Expressed as in Table 3

Airflow Rate (mL/min)	Trial	Percentage of Dose					
		0.5 h	1 h	2 h	4 h	6 h	8 h
10	I	15.2	18.8	10.7	2.7	0.60	0.24
	II	11.0	22.8	14.8	5.4	1.1	0.37
20	I	14.9	12.2	5.2	1.3	0.35	0.17
	II	9.9	15.9	9.2	2.6	0.59	0.21
30	I	5.0	7.8	5.7	1.7	0.26	0.09
	II	6.9	8.9	6.4	2.1	0.42	0.12
40	I	5.5	5.9	3.1	1.0	0.18	0.07
	II	7.0	9.1	6.0	2.3	0.43	0.15
50	I	4.2	3.7	2.3	0.65	0.13	0.05
	II	6.1	5.6	2.4	0.62	0.13	0.06
65	I	5.5	4.2	2.0	1.0	0.45	0.27
	II	5.5	4.8	2.7	0.81	0.18	0.07
80	I	3.3	3.9	2.5	0.77	0.16	0.07
	II	5.5	6.1	3.8	1.2	0.25	0.10
100	I	6.0	4.0	2.0	0.51	0.12	0.05
	II	5.5	3.9	1.7	0.54	0.11	0.04

attributed in part to a lag time for vapor collection resulting from the finite headspace (~4 mL) between the skin surface and the vapor trap. The initial low benzyl alcohol concentration, and correspondingly low chemical potential, may also have contributed to this effect. It seemed unwise to attempt to model this effect on the basis of such limited data; hence, the 0–5 min values have been omitted from the regression analysis described below. A second trend, also evident in Figure 4, was that the absorption rate plots were nearly log linear after an initial time lag, whereas the evaporation rate plots were concave with respect to the top of the figure. Both of these trends can be qualitatively described using the two-compartment models, Models 2 and 3, as shown below. They cannot be described by Model 1, which leads to a single exponential decay rate for both evaporation and absorption.

Fit of Pharmacokinetic Models to Experimental Data

The rate constants for Models 1–3 were fit to the experimental data in Tables 3 and 4 as described in the Experimental section. The results of this analysis are shown in Table 2. The linear evaporation model represented by eq. (6) yielded slightly better fits than eq. (7) and was therefore selected for this analysis. The cumulative percentages of benzyl alcohol evaporated and absorbed after 8 h were adequately described by all three of the pharmacokinetic models. This may be seen by examining the long-time skin disposition plots in Figure 3. There was some evidence of systematic deviations of the model predictions from the experimental data, indicating that the dependence of evaporation rate on airflow may be more complex than that given in eq. (6). These deviations were not reduced by the substitution of eq. (7) for eq. (6) or by the addition of a second compartment (Models 2 and 3).

Substantial differences were found in the ability of the three pharmacokinetic models to describe the time course of evaporation and absorption. Examples are shown in Figure 4. Model 1, which yields a single exponential decay rate and no time lag for absorption through the skin, clearly missed the details of both the evaporation and absorption processes. The two-compartment models were somewhat better in this respect. Models 2 and 3 lead to a biexponential decay for evaporation rate and a time lag for skin absorption. We found that Model 2 yielded more consistent matches to the evaporation rate plots than did Model 3. However, both models failed to accurately describe the pronounced "tail" of the evaporation rate plots (and, to a lesser extent, the absorption rate plots) at long values of the time. In other words, the evaporation rate of benzyl alcohol from the skin at long times was higher than predicted by the compartmental models. Although these differences could presumably be reduced by weighting them more heavily in the regression analysis, such

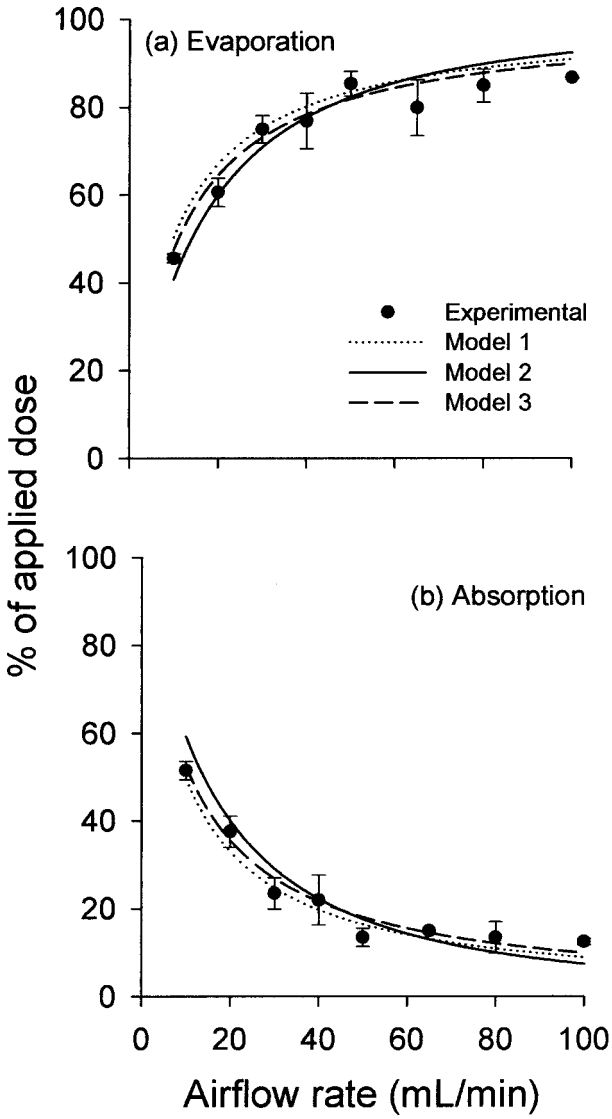

Figure 3. Correlations of (a) total percentage of benzyl alcohol evaporated, and (b) total percentage absorbed versus surface airflow.

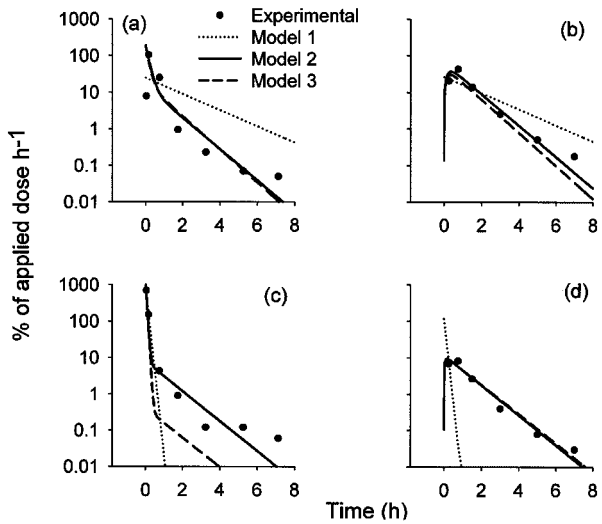

Figure 4. Evaporation and absorption rate plots of benzyl alcohol *in vitro* (data from Trial I): (a) evaporation (10 mL/min), (b) absorption (10 mL/min), (c) evaporation (80 mL/min), and (d) absorption (80 mL/min).

improvements would come at the expense of accuracy in the cumulative evaporation and absorption estimates. This may be seen qualitatively by noting that slopes of the evaporation rate curves in Figure 4 change continuously rather than bilinearly with time.

The regression statistics in Table 2 (s, r^2, χ_v^2) indicate that Model 3 yielded slightly better fits to the combined datasets than did Models 1 and 2, using the sequentially determined parameter values reported in the table. The differences are significant ($p < 0.05$ for Model 3 versus either Model 1 or 2) based on an F-test of the χ_v^2 ratios.[23]

This does not negate the fact that Model 2 more consistently described the evaporation rate data for individual datasets. Each of the three models has certain strengths, yet none of them provided a complete description of the data. Their utility ultimately hinges on their predictive power in other situations.

DISCUSSION

The kinetic analysis for benzyl alcohol disposition on skin presented here builds on an earlier analysis of *in vivo* skin disposition of a multicomponent fragrance mixture.[7] In the previous study, only evaporation data were available and the data were collected at a single airflow rate. Thus, it was not possible to verify absorption rates or to test the airflow dependence [eqs. (6) and (7)]. The present study focuses on these factors. Because only a single compound was tested, it was not possible here to confirm the physical properties dependencies of the rate constants proposed earlier [eqs. (2) and (3)]. A comprehensive model of fragrance disposition on skin must combine these factors along with skin temperature and a defensible range of exposure conditions.[7] Considerable work remains in order to reach this objective. The investigators envision that a deterministic model of the nature described here can be combined stochastically with exposure variables

such as wind velocity, temperature, body site, and skin condition to produce improved dermal absorption estimates for fragrance ingredients and other volatile organic compounds that transiently contact skin.

The question of ingredient interactions deserves further attention. The present analysis, including the multicomponent mixture analysis in Ref. 7, does not explicitly consider such interactions; thus, each component is assumed to diffuse and evaporate independently. This is clearly an oversimplification of the physical situation, as thermodynamic activity of each component depends on the composition of the milieu in which it resides. In a true diffusion model, these activities could be calculated as the product of local concentration and activity coefficient of each component. Activity coefficients for fragrance ingredients and other small organic compounds in pharmaceutical systems have been successfully estimated using engineering methods such as UNIFAC and UNIQUAC.[24,25]

In anticipation of these developments, we tested one implementation of the activity coefficient correction for the present dataset, in which benzyl alcohol was applied to skin in ethanolic solution (data not shown). Evaporation and absorption rate constants for ethanol were estimated from those of benzyl alcohol using eqs. (2) and (3) and the appropriate ratios of physical properties. Activity coefficients in the vehicle and skin compartments were estimated from their current composition using the UNIFAC/UNIQUAC method.[24] To do this, the skin compartment was assumed to contain 0.15 mg/cm^2 of a lipid mixture having the chemical properties of *n*-octanol.[3,4] Activity coefficients thus calculated were used as multipliers for the evaporation and absorption rate constants in eqs. (A.1), (A.2), (A.9), and (A.10), and the rate equations were integrated numerically to produce corrected values of A_{air} and A_{bl}. These values were then compared with the observed evaporation and absorption values in Tables 3 and 4 and the rate constants were optimized by least squares.

Despite the considerable expenditure of time and energy, no significant improvements in fits to modeling the benzyl alcohol evaporation and absorption data were obtained by this process relative to the linear model results in Table 2. Therefore, this particular approach based on corrections to linear pharmacokinetic models cannot be recommended. However, it seems probable that careful implementation of this methodology in the context of a true diffusion model, in combination with experimental observations on more than one component, would lead to more satisfactory results. This seems a promising area for further study.

CONCLUSIONS

Benzyl alcohol disposition on skin *in vitro* after topical application in ethanol is significantly influenced by airflow over the skin surface. A one-compartment, first-order kinetic model with an airflow-dependent evaporation rate constant (Model 1) provides a satisfactory description of the evaporated and absorbed fractions several hours post-dose. More details of the absorption and evaporation curves can be accounted for using two-compartment models (Model 2 and 3) that explicitly consider the initial dry down process on skin. With additional calibration from other compounds and *in vivo* exposures, these models may have value for predicting the disposition of volatile chemicals having transient contact with the skin. The two-compartment models have better prospects for describing the changing composition of vapors arising from the skin surface after topical application of complex mixtures, as would be important for a quantitative description of fragrance evolution.

ACKNOWLEDGMENTS

The authors thank Dr. Pedro Rodriguez for advice on the vapor trapping methodology. P.S. thanks the University of Cincinnati for a Distinguished Dissertation fellowship. This work was supported by the Procter and Gamble Company's International Program for Animal Alternatives, the University of Cincinnati, and NIOSH grant 1 RO1 OH007529-01.

APPENDIX

Solutions to Two-Compartment Skin Disposition Models

The models shown schematically in Figure 1 are analyzed as follows. Ingredient levels are expressed as the amount of material in each compartment, A, at time t.

Model 1 (Fig. 1a)

See eqs. (1)–(5) and Ref. 7.

Model 2 (Fig. 1b)

The rate equations for this scenario are:

$$\frac{dA_{veh}}{dt} = -(k_1 + k_2)A_{veh} \quad (A.1)$$

$$\frac{dA_{skin}}{dt} = k_2 A_{veh} - (k_3 + k_4)A_{skin} \quad (A.2)$$

These equations are integrated subject to the initial condition $A_{veh}(0) = A_0$; $A_{skin}(0) = 0$. Because A_{veh} does not depend on A_{skin}, eqs. (A.1) and (A.2) can be solved sequentially and the exponential decay constants for the vehicle and skin compartments are not coupled. The integrated equations are:

$$A_{air}(t) = \frac{A_0}{\alpha\beta(\beta - \alpha)}\{[k_1\beta(\beta - \alpha) + k_2k_4\beta](1 - e^{-\alpha t}) - k_2k_4\alpha(1 - e^{-\beta t})\} \quad (A.3)$$

$$A_{veh}(t) = A_0e^{-\alpha t} \quad (A.4)$$

$$A_{skin}(t) = k_2A_0\left[\frac{1}{\beta - \alpha}\right](e^{-\alpha t} - e^{-\beta t}) \quad (A.5)$$

$$A_{bl}(t) = \frac{k_2k_3A_0}{\alpha\beta(\beta - \alpha)}[\beta(1 - e^{-\alpha t}) - \alpha(1 - e^{-\beta t})] \quad (A.6)$$

where $\alpha = k_1 + k_2$ and $\beta = k_3 + k_4$.

After a long time ($t \to \infty$), the amount of ingredient in the air and the amount of ingredient absorbed into blood circulation can be expressed as

$$A_{air}(\infty) = \frac{A_0}{\alpha\beta}(k_1k_4 + k_1k_3 + k_2k_4) \quad (A.7)$$

and

$$A_{bl}(\infty) = \frac{A_0}{\alpha\beta}(k_2k_3) \quad (A.8)$$

where $\alpha\beta = k_1k_4 + k_1k_3 + k_2k_4 + k_2k_3$.

Model 3 (Fig. 1c)

The rate equations for this model are

$$\frac{dA_{veh}}{dt} = -(k_1 + k_2)A_{veh} + k_{-2}A_{skin} \quad (A.9)$$

$$\frac{dA_{skin}}{dt} = k_2A_{veh} - (k_{-2} + k_3)A_{skin} \quad (A.10)$$

and the initial conditions are $A_{veh}(0) = A_0$; $A_{skin}(0) = 0$.

The equations are solved simultaneously using Laplace transforms. The integrated equations are

$$A_{air}(t) = \frac{k_1A_0}{\alpha\beta(\beta - \alpha)}[(k_{-2} + k_3 - \alpha)\beta(1 - e^{-\alpha t}) + (\beta - k_{-2} - k_3)\alpha(1 - e^{-\beta t})] \quad (A.11)$$

$$A_{veh}(t) = \frac{A_0}{\beta - \alpha}[(k_{-2} + k_3 - \alpha)e^{-\alpha t} + (\beta - k_{-2} - k_3)e^{-\beta t}] \quad (A.12)$$

$$A_{skin}(t) = \frac{k_2A_0}{\beta - \alpha}\left[e^{-\alpha t} - e^{-\beta t}\right] \quad (A.13)$$

$$A_{bl}(t) = \frac{k_2k_{-2}A_0}{\alpha\beta(\beta - \alpha)}[\beta(1 - e^{-\alpha t}) - \alpha(1 - e^{-\beta t})] \quad (A.14)$$

where

$$\alpha = \frac{1}{2}\left[\alpha + \beta + \sqrt{(\alpha + \beta)^2 - 4\alpha\beta}\right]$$

$$\beta = \frac{1}{2}\left[\alpha + \beta - \sqrt{(\alpha + \beta)^2 - 4\alpha\beta}\right]$$

$$\alpha + \beta = k_1 + k_2 + k_{-2} + k_3$$

$$\alpha\beta = k_1k_{-2} + k_1k_3 + k_2k_{-2}.$$

After a long time ($t \to \infty$), the amount of ingredient in the air and the amount absorbed into blood circulation can be expressed as

$$A_{air}(\infty) = \frac{k_1A_0}{\alpha\beta}(k_{-2} + k_3) \quad (A.15)$$

and

$$A_{bl}(\infty) = \frac{k_2k_{-2}A_0}{\alpha\beta} \quad (A.16)$$

REFERENCES

1. Gerberick GF, Robinson MK. 2000. A skin sensitization risk assessment approach for evaluation of new ingredients and products. Am J Contact Dermat 11:65–73.
2. Robinson MK, Gerberick GF, Ryan CA, McNamee P, White I, Basketter DA. 2000. The importance of exposure estimation in the assessment of skin sensitization risk. Contact Dermatitis 42:251–259.
3. Wilschut A, ten Berge WF, Robinson PJ, McKone TE. 1995. Estimating skin permeation. The validation of five mathematical skin penetration models. Chemosphere 30:1275–1296.

4. Potts RO, Guy RH. 1992. Predicting skin permeability. Pharm Res 9:663–669.
5. Cleek RL, Bunge AL. 1993. A new method for estimating dermal absorption from chemical exposure. I. General approach. Pharm Res 10:497–506.
6. Kasting GB. 2001. Kinetics of finite dose absorption. I. Vanillylnonanamide. J Pharm Sci 90:202–212.
7. Kasting GB, Saiyasombati P. 2001. A physicochemical properties based model for estimating evaporation and absorption rates of perfumes from skin. Int J Cosmet Sci 23:49–58.
8. Vuilleumier C, Flament I, Sauvegrain P. 1995. Headspace analysis study of evaporation rate of perfume ingredients applied onto skin. Int J Cosmet Sci 17:61–76.
9. Bronaugh RL, Wester RC, Bucks DAW, Maibach HI, Sarason R. 1990. *In vivo* percutaneous absorption of fragrance ingredients in rhesus monkeys and humans. Food Chem Toxicol 28:369–373.
10. Barry BW, Harrison SM, Dugard PH. 1985. Correlation of thermodynamic activity and vapour diffusion through human skin for the model compound, benzyl alcohol. J Pharm Pharmacol 37: 84–90.
11. Barry BW, Harrison SM, Dugard PH. 1985. Vapour and liquid diffusion of model penetrants through human skin: Correlation with thermodynamic activity. J Pharm Pharmacol 37:226–235.
12. Jimbo Y, Isihara M, Osamura H, Takano M, Ohara M. 1983. Influence of vehicles on penetration through human epidermis of benzyl alcohol, isoeugenol, and methyl isoeugenol. J Invest Dermatol 10:241–250.
13. Menczel E, Maibach HI. 1970. *In vitro* human percutaneous penetration of benzyl alcohol and testosterone: Epidermal-dermal retention. J Invest Dermatol 54:386–394.
14. Consumers TSCoCPaN-fPIf. 1999. Fragrance allergy in consumers: A review of the problem.
15. McCarley KD, Bunge AL. 2001. Pharmacokinetic models of dermal absorption. J Pharm Sci 90:1699–1719.
16. Wagner JG. 1979. Fundamentals of clinical pharmacokinetics. Hamilton, IL: Drug Intelligence Publications.
17. Saiyasombati P. 2003. Mathematical model for predicting the percutaneous absorption of fragrance raw materials [PhD thesis]. Cincinnati, OH: University of Cincinnati, College of Pharmacy.
18. Meylan W. 1999. MPBPVP. North Syracuse, NY: Syracuse Research Corporation.
19. Yalkowski SH. 1993. AQUASOL database. Tucson, AZ: University of Arizona.
20. Hansch C, Leo A. 1999. MEDCHEM database and CLOGP. Claremont, CA: BioByte, Inc.
21. Merritt EW, Cooper ER. 1984. Diffusion apparatus for skin penetration. J Control Release 1:161–162.
22. Kasting GB, Filloon TG, Francis WR, Meredith MP. 1994. Improving the sensitivity of *in vitro* skin penetration experiments. Pharm Res 11:1747–1754.
23. Bevington PR. 1969. Data reduction and error analysis for the physical sciences. New York: McGraw-Hill.
24. Reid RC, Prausnitz JM, Poling BE. 1987. The properties of liquids and gases. New York: McGraw Hill.
25. Tse G, Blankschtein D, Shefer A, Shefer S. 1999. Thermodynamic prediction of active ingredient loading in polymeric microspheres. J Control Release 60:77–100.